International Journal of Fluid Machinery and Systems
Vol. 4, No. 1, January-March 2011

DOI: 10.5293/IJFMS.2011.4.1.133
ISSN (Online): 1882-9554

Original Paper (Invited)

Numerical Design and Performance Prediction of Low Specific Speed Centrifugal Pump Impeller

Zhang Yongxue, Zhou Xin, Ji Zhongli and Jiang Cuiwei

Faculty of Mechanical and Electronic Engineering, China University of Petroleum-Beijing
Beijing, 102249, China
zhyx@cup.edu.cn, zhouxin_928@163.com,
jizl@tsinghua.org.cn, jiangcuiwei123@163.com

Abstract

In this paper, Based on Two-dimensional Flow Theory, adopting quasi-orthogonal method and point-by-point integration method to design the impeller of the low specific speed centrifugal pump by code, and using RANS (Reynolds Averaged N-S) Equation with a standard k-ε two-equation turbulence model and log-law wall function to solve 3D turbulent flow field in the impeller of the low specific speed pump. An analysis of the influences of the blade profile on velocity distributions, pressure distributions and pump performance and the investigation of the flow regulation pattern in the impeller of the centrifugal pump are presented. And the result shows that this method can be used as a new way in low speed centrifugal pump impeller design.

Key words: Low Specific Speed, Centrifugal Pump impeller, Two-dimensional Flow Theory, Numerical Design，Performance Prediction

1. Introduction

Centrifugal pump is the most widely used vane pump, and a wide variety of centrifugal pump types are used in many different applications in industry and other technical sectors. After long-term research and practice in centrifugal pump, a wealth of experience of slope of head-capacity characteristic curve which bring about low flow rate instability and high flow rate power overload [1]. Traditional impeller design methods, which are mainly based on the similarity theory, empirical correlation, combination of model testing, and engineering experience, their design process are difficult task, mainly due to the great number of free geometric parameters. [2, 3, 4] So well hydraulic design of low specific pump impeller becomes more difficult and more necessary. Regardless of the design process used, the final decision of a new pump impeller design is usually made following physical testing. These tests are often time and resources consuming. In addition, the flow field in impeller channels is very complicated, so that no simple mathematic model can be established to well predict the performance of impellers. For these reasons CFD (computational fluid dynamics) analysis is currently being carried out on centrifugal impeller. [5, 6, 7, 8] By using it can provide quite accurate information on the fluid behaviour, and thus helps the engineers to obtain a thorough performance evaluation of the design.

In this paper, based on Two-dimensional flow theory low specific speed pump impeller design method, which adopting quasi-orthogonal method and point-by-point integration, is put forward. 3D turbulent flow field in the designed impeller is calculated numerically by using RANS (Reynolds Averaged N-S) Equation with standard k-ε turbulence model and log-law wall function. And predicting result of impeller according to the flow is presented.

2. Hydraulic design of impeller

2.1 Design of the meridional section

First, determine the geometrical features (D_1, D_2, B_2, Z, etc.) of the impeller, according to the given set of operating conditions (usually Q, H, n, available NPSH, etc.) by empirical correlation. Then, for low specific speed centrifugal pump impeller with long narrow flow channels, in order to convenience and simple of programming and modifying of some parameters, select line and transition arc to draw the initial meridional section profile. For impellers with an axial inlet, the angle (between inlet edge and shaft

Accepted for publication December 23, 2010: Paper number O10057S
Corresponding author: Zhang Yongxue, Professor, zhyx@cup.edu.cn
This paper was presented at 2010 International Conference on Pumps and Fans, October 18-21, 2010, Hangzhou, China

direction, 30-40 degree) is about the optimum according to [9]. If the angle is too small, problems with hub cavitations and instabilities of head-capacity characteristic curve may be encountered. If choosing too large, this may result in too large blade angles on the hub.

2.2 Calculation of meridional flow

Calculate the flow of meridional section by quasi-orthogonal method. This method is to establish the quasi-orthogonal gradient equation of meridional component of absolute speed and solve it by iterative calculation to get meridional velocity at each point. [10]

The equation:

$$\frac{dC_m}{ds}=C_m\left[\left(\frac{d\alpha_1}{ds}-\frac{\partial\alpha_1}{\partial l}\sin\delta\right)\frac{1}{\cos\delta}-\frac{\sin\alpha_1}{r}-\frac{\partial\ln\psi}{\partial l}\right]\sin\delta+K\cos\delta \tag{1}$$

The value of parameter K should be given to solve the equation to get meridional velocity C_m. When we let $K=-kC_m\frac{d\alpha_1}{dl}$, then the equation will express One-dimensional Flow Theory design at the condition $k=0$, Two-dimensional Flow Theory design with $\Omega_u=0$ at the condition $k=1$ and Two-dimensional Flow Theory design with $\Omega_u\neq 0$ at the condition $k\in(0,1)$. The relation of quasi-orthogonal, streamline and cross section line is shown in Fig.1.

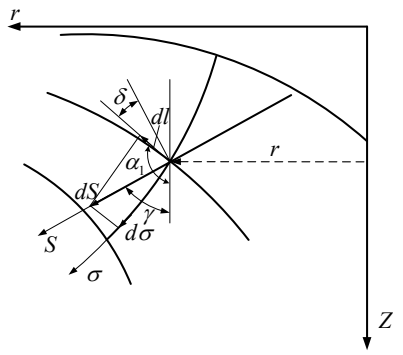

Fig. 1 Relation of quasi-orthogonal, streamline and across section line

2.3 Meridional profile adjustments

Since flow cross-section lines are perpendicular to meridional streamlines, after the calculation of meridional flow, the slope on streamlines at each point can achieve and then cross-section lines can get. To check the meridional profile qualified or not, by examining the flow cross-section areas distribution along the meridional streamline. If not, adjust the meridional profile and re-calculate.

The adjust method is: assuming the required areas distribution is $S=f(l)$ and the calculated value is S', former profile point is $p_0\ (r_0,Z_0)$ and the after adjusting is $p_1\ (r_1,Z_1)$. When the distance between p_0 and p_1 is small, it can be considered that p_1 is on the tangential direction of the cross-section line at former point p_0 ,shown as Fig.2.Then equation about the area difference $\Delta S=S-S'$ and position of p_1 can set up.

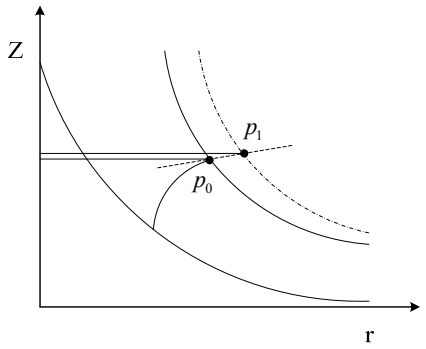

Fig. 2 Meridional profile adjustments

2.4 Blade drawing

When assuming impeller has infinite number of blades, the camber lines of blades and streamlines are coincided. After given the relationship of blade wrapping angle and length of meridional streamline, camber lines can be obtained by solving the integral of the equation:

$$\varphi = \int_0^l \frac{1}{r} \sqrt{\frac{W^2}{C_m^2} - 1} dl \tag{2}$$

2.5 Blade leading and trailing edge smoothing

The geometry of the leading edge plays an important role in the blade design process. It will affect the anti-cavitations performance of the impeller, especially for low specific speed centrifugal pump impeller. The discontinuities of the leading and trailing edge can be easily defined using curve approximation techniques. Traditional filleting method can smooth the blade at leading edge, but cannot modify to meet different requirement. So Bezier curve line is adopted to smooth the blade leading edge, which can be described in simple and flexible manner and allow for correcting the control point locations according to different conditions. [11] The smoothing method is shown in Fig.3.

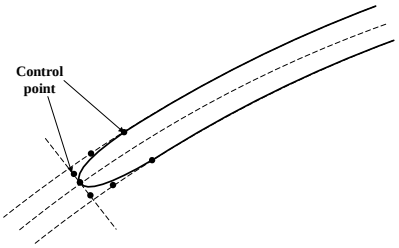

Fig. 3 Leading edge of blade smoothing

3. Numerical simulations

3.1 Geometry and Grid

Use the method mentioned above, a pump impeller (Flow rate $Q = 45.68\text{m}^3/\text{h}$, Head $H = 46.41\text{m}$, Rotate speed $n = 2900\,\text{r/min}$) has designed with parameters as $D_j = 66\text{mm}$, $b_2 = 9\text{mm}$, $D_2 = 202\text{mm}$ and $Z = 5$ .The impeller model is shown in Fig.4.

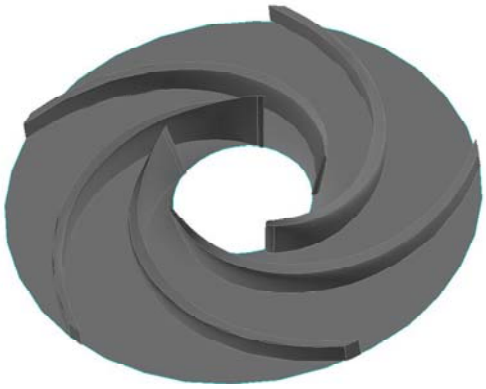

Fig. 4 Impeller model

The calculation domain is mainly composed of two parts, the static component and the rotating impeller. The discretization of the geometry is done keeping the balance between calculation time and the accuracy order of the simulation of the flow structure. And it is generated by the GAMBIT pre-process code, and un-structure tetrahedral grid with strong flexibility is adopted for the mesh. The computational region and grids are shown in Fig.5.

Fig. 5 Computational gird

3.2 Flow Calculate

Supposing the fluid is viscous and incompressible, the simulation is conducted by applying uncompressible mass conservation equations, and Reynolds Averaged Navier-Stokes equations as well as the standard k- ε turbulent model which is implemented on

commercial code (FLUENT). [12] For such calculations, wall functions, based on the logarithmic law, have been used. The pressure-velocity coupling is calculated through the SIMPLEC algorithm. Second order, upwind discretizations have been used for convection terms and PRESTO! for pressure terms.

3.3 Boundary Conditions

Inlet boundary condition is the velocity inlet and assumed as a uniform velocity distribution. In the present work, the absolute velocity in the axial direction is assumed to be uniform and its magnitude is computed from the specified flow rate. The magnitudes of the absolute velocity vectors in radial and tangential directions are assumed to be zero. Outlet the outflow is given as boundary condition. The solid wall such as blade surface, hub and shroud is given the moving wall and non-slip condition. The flow rate is changed by modifying the velocity magnitude at the inlet.

4. Performance prediction

4.1 Head calculation

The energy H gained by the fluid through the impeller, is computed from the total energy of the fluid at the inlet and outlet of the impeller: [13]

$$H = H_2 - H_1 = \frac{1}{Q} \cdot \int \left(\frac{p_2 - p_1}{\rho g} + \frac{c_2^2 - c_1^2}{2g} \right) \cdot dq \tag{3}$$

Where the right-hand side integral can be approximated by a summation over the radial flow rates dq at all grid cells facing at inlet or outlet of the impeller.

4.2 Hydraulic efficiency calculation

The hydraulic efficiency of the impeller is defined as the ratio of the net energy (H) added to the passing fluid, divided by the energy (H_u) given at the impeller shaft. And H_u can be calculated from the torque M_u developed on the blades:

$$H_u = \frac{\omega \cdot M_u}{\rho \cdot g \cdot Q} = \frac{\omega \cdot \int \left[(\vec{r} \times \vec{n}) \cdot p + (\vec{r} \times \vec{\tau}_w) \cdot \cot \beta \right] \cdot b \cdot dr}{\rho \cdot g \cdot Q} \tag{4}$$

So the hydraulic efficiency of the impeller can be finally defined as:

$$\eta = \frac{H}{H_u} \tag{5}$$

5. Simulation results and analysis

The distribution of the relative velocity and pressure in impeller channels, the performance of impellers are determined by its structural parameter, geometrical shape, rotational speed, capacity, inlet and outlet condition.

The simulation results of the relative velocity and pressure are obtained at rotating speed n = 2900 rpm and flow rate at 0.6Q, 0.8Q, Q, 1.2Q and 1.4Q.

5.1 Relative Velocity

When the capacity $Q = 45.68 \mathrm{m}^3/\mathrm{h}$, the relative velocity contours between blades at different value of d/D_2 (0.4, 0.6, 0.8, 1.0) are shown in Fig.6.(a)-(d). And Fig.7 shows there relative positions and relative velocity distribution on the impeller.

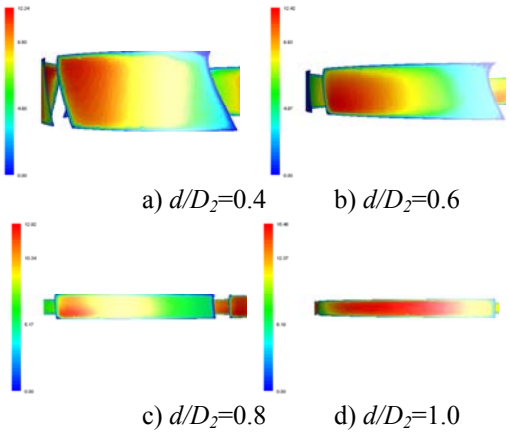

a) d/D_2=0.4 b) d/D_2=0.6

c) d/D_2=0.8 d) d/D_2=1.0

Fig. 6 Distribution of relative velocity at different diameters (m/s)

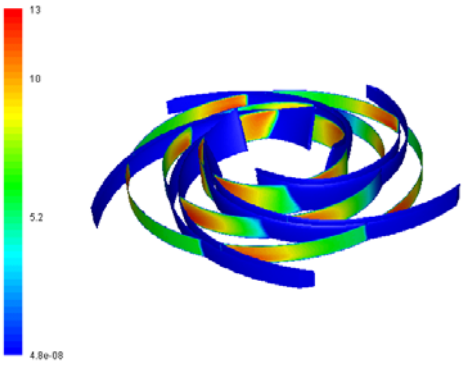

Fig. 7 Distribution of relative velocity (m/s)

From these Figures, it can be seen that the relative velocity at the suction side of the blade is larger than pressure side at the same diameters. At d/D_2=0.4, the maximum value is located at the junction of suction side and shroud. As the fluid move along the passage, the location of the maximum value changes from shroud side to hub and the relative velocity come to be more uniform.

5.2 Static Pressure

When the capacity $Q = 45.68\text{m}^3/\text{h}$, the static pressure contours between blades at different value of d/D_2 (0.4, 0.6, 0.8, 1.0) are shown in Fig.8.(a)-(d). And Fig.9 shows there relative position and pressure distribution on the impeller.

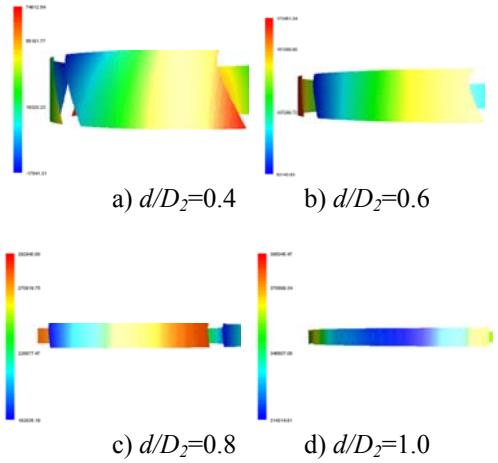

a) d/D_2=0.4 b) d/D_2=0.6

c) d/D_2=0.8 d) d/D_2=1.0

Fig. 8 Distribution of static pressure at different diameters (Pa)

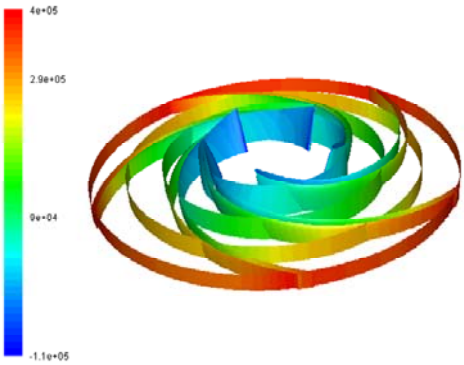

Fig. 9 Distribution of static pressure (Pa)

As it can be seen from the above Figures, the static pressure on the pressure side is larger than that on the suction side. The minimum value exists at the junction of suction side and shroud, and the maximum value exists at the junction of pressure side and hub. As the fluid move along the passage, the pressure values get enlarged and pressure distribution becomes more uniform.

From Fig.(10). and Fig.(11) , it can be seen that, the pressure is enlarged uniformly from leading edge to the trailing But at the outlet of the impeller, there exists local non-uniform pressure distribution, which may cause energy loss.

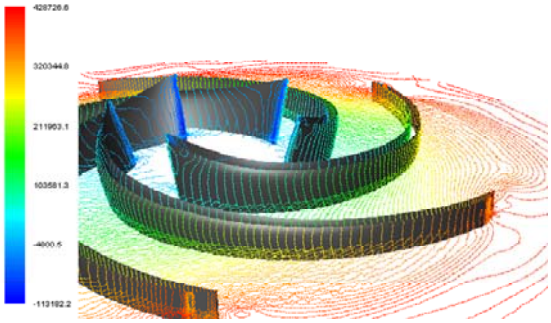

Fig. 10 Distribution of static pressure on the blade (Pa)

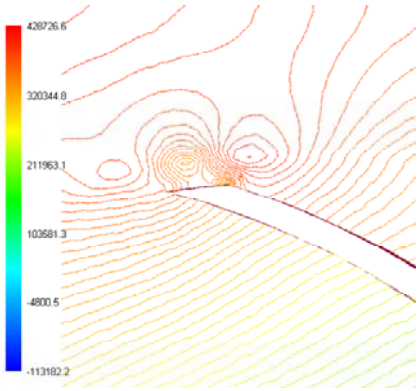

Fig. 11 Distribution of static pressure near the trailing edge (Pa)

5.3 Hydraulic Performance

After computational of different flow rate condition of the impeller, the head and hydraulic efficiency data of the impeller calculated by the above mention method are draw on the Fig.(12).

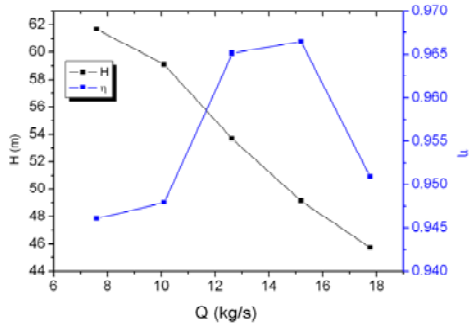

Fig. 12 Hydraulic performance of the impeller

It can be seen from the figure that, the slope of head curve is always negative, which is good for the stability of the impeller running. The highest efficiency point on the calculate data is at 1.2Q and the lowest efficiency point is at 0.6Q. And the difference between the highest and lowest efficiency value is about 2% in the range of the calculation.

6. Conclusions

A new numerical hydraulic design method of low specific centrifugal pump impeller which can combine computer technology to realize a fast design and optimization is promoted. With commercial code, the performances of impeller are predicted according to the computational result of flow in the impeller passage. The use of CFD performances prediction can reduce physical testing. And the result shows that this design method is available.

Acknowledgments

The research is supported by National Natural Science Foundation of China (project No: 50809075). The supports are highly appreciated.

Nomenclature

D_1	Blade inlet diameter[mm]	D_2	Blade inlet diameter[mm]
B_2	Width of impeller at outlet[mm]	Z	Blade number of impeller
Q	Capacity [m^3/h]	H	Head(m)
n	Rotate speed [r/min]	C_m	Meridional velocity[m/s]
s	Length of quasi-orthogonal line[mm]	α_1	Angle between meridional streamline and vertical line[°]
δ	Angle between normal line of quasi-orthogonal line and meridional streamline[°]	ψ	Expelling coefficient
		γ	Angle between quasi-orthogonal line and axis[°]
l	length of meridional streamline[mm]	W	Relative velocity[m/s]
φ	Wrapping angle[°]	P_2	Static pressure at outlet[Pa]
P_1	Static pressure at inlet[Pa]	C_2	Absolute velocity at outlet[m/s]
C_1	Absolute velocity at inlet[m/s]	g	Gravity[kg m/s^2]
ρ	Density	D_j	Blade eye diameter[mm]
β	Blade set angle[°]	ω	Angle velocity
M_u	Torque	$\vec{\tau}_w$	Wall shear stress
$\vec{n}$	Unit vector normal to blade surface		

References

[1] Peng Xiao-qiang, Zhang Yong-xue, Cao Shu-liang, 2004, "Numerical-analysis of 3D Turbulent Flow in a Low Specific Speed Pump Impeller," Transactions of the Chinese Society of Agricultural Machinery, Vol. 35, No. 1, pp. 69-72.

[2] Yang Jun-hu, 2002, "Flow Mechanism inside the Impeller of a Centrifugal Pump with Low Specific Speed and Design of the Impeller," Transactions of the Chinese Society of Agricultural Machinery, Vol. 33, No. 2.

[3] Qi Xue-yi, Hu Jia-xin, Tian Ya-bin, 2009, "Orthogonal design of complex impeller of centrifugal pump with super-low-specific-speed," Drainage and Irrigation Machinery, Vol. 27, No. 5, pp. 341-346.

[4] Ni Yong-yan, Yuan Shou-qi, Yuan Jian-ping, 2008, "Model of enlarged flow design for low specific speed centrifugal pump," Drainage and Irrigation Machinery, Vol. 26, No. 1, pp. 21-24.

[5] Wang Yang, He Wen-jun, 2009, "Improved Attempt of Non-overload Centrifugal Pumps Based on Fluent," Transactions of the Chinese Society of Agricultural Machinery, Vol. 40, No. 9, pp. 85-88.

[6] Yuan Shouqi, Ni Yongyan, Pan Zhongyong, 2009, "Unsteady Turbulent Simulation and Pressure Fluctuation Analysis for Centrifugal Pumps," Chinese Journal of Mechanical Engineering, Vol. 22, No. 1, pp. 64-69.

[7] John S. Anagnostopoulos., 2006 "CFD Analysis and Design Effects in a Radial Pump Impeller," Wseas Transactions of Fluid Mechanics, Vol. 1, No. 7, pp. 763-770.

[8] José González Pérez, Carlos Santolaria Morros., 2006, "Unsteady Flow Structure and Global Variables in a Centrifugal Pump," ASME Jouranl of Fluids Engineering, Vol. 128, pp. 937-946.

[9] Güich J F.,2008, Centrifugal Pumps,. Heidelberg: Springer Berlin Heidelberg, .

[10] Cao Shu-liang, Liang Li, Zhu Bao-shan, 2005, "Design method for impeller of high specific speed mixed-flow pump," Journal of Jiangsu University(Natural Science Edition), Vol. 26, No. 3, pp. 185-188.

[11] Vasilios A. Grapsas, John S., 2005, "Anagnostopoulos, Dimitrios E. Papantonis. Hydrodynamic Design of Radial Flow Pump Impeller by Surface Parameterization," 1st International Conference on Experiments / Process / System Modelling / Simulation / Optimization , GT-2005.

[12] Zhang Shujia, Li Xianhua, Zhu Baolin, 2009, "Applicability of k-εEddy Viscosity Turbulence Models on Numrical Simulation of Centrifugal Pump," Journal of Mechanical Engineering, Vol. 45, No. 4, pp. 238-242.

[13] Suthep Kaewnai, Manuspong Chamaoot, Somchai Wongwises., 2009, "Predicting performance of radial flow type impeller of centrifugal pump using CFD," Journal of Mechanical Science and Technology, Vol. 23, pp. 1620-1627.